

1 Supplement of “Evaluation of the quality of a UAV-based eddy 2 covariance system for measurements of wind and turbulent flux”

3 Yibo Sun¹, Xinwen Lin⁴, Bing Geng⁵, Bo Liu^{1,2,3}, Shennan Ji^{1,2,3}

4 ¹State Key Laboratory of Environmental Criteria and Risk Assessment, Chinese Research Academy of Environmental
5 Sciences, Beijing 100012, China.

6 ²Institute of Ecology, Chinese Research Academy of Environmental Sciences, Beijing 100012, China.

7 ³State Environmental Protection Key Laboratory of Ecological Regional Processes and Functions Assessment, Beijing
8 100012, China.

9 ⁴Collage of Geography and Environment Science, Zhejiang Normal University, Zhejiang 321004, China

10 ⁵Beijing Academy of Social Sciences, 100101, Beijing, China.

11 *Correspondence to:* Yibo Sun (sunyb68@163.com)

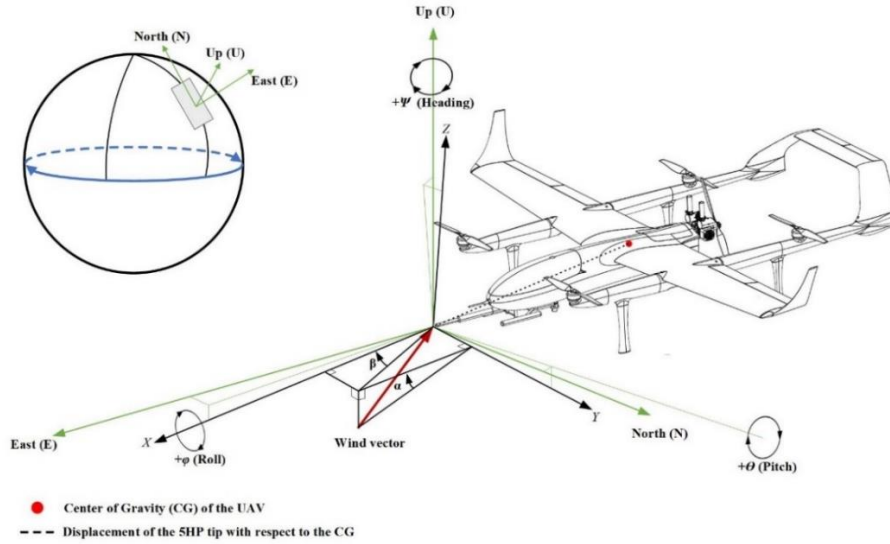
12 The intention of this supplement is to guide the readers through the relevant equations about geo-referenced wind calculation,
13 and to provide the procedures in calibration the mounting misalignment using data from ‘box’ maneuver. Section 1 provides
14 the formulas necessary to compute the geo-referenced 3D wind vector. Section 2 provides the procedure and results for
15 calibrating the mounting misalignment based on ‘box’ flight maneuver. References to literature are given at the end of the
16 document.

17 **1 Detailed equations for calculation of the geo-referenced 3D wind vector**

18 Wind measurement by aircraft is challenging. The wind measurement components of the UAV-based EC system consist of
19 sensors that measure air pressure (static and dynamic pressure), air temperature, and aircraft attitude, position, velocity, and
20 angular velocity. From these measurements, two velocity vectors U_a (velocity of the air with respect to the aircraft) and U_p
21 (velocity of the aircraft with respect to the Earth) are derived. The velocity of the wind with respect to the earth U (i.e., geo-
22 referenced wind vector) is the result of adding these two vectors together, as:

$$23 \quad U = U_a + U_p \quad (S1)$$

24 For a fixed-wing aircraft, approaches to compute the geo-referenced wind vector based on the combination of a multi-hole
25 probe and navigation system are often similar in principle. This text provides the basic formulas necessary to compute the
26 geo-referenced wind vector measured from an aircraft. Detailed information about airborne wind measurement is found in
27 the literature (e.g., Crawford and Dobosy (1992); Williams and Marcotte (2000); Khelif et al. (1999); Metzger et al. (2011)).
28 Figure S1 illustrates the transformational relation for the geo-referenced wind vector calculation used by the current UAV-
29 based EC system.



30

31 **Figure S1. Diagram of the coordination transformational relation for geo-referenced wind vector calculation. The green**
 32 **coordinate represents the geo-referenced coordinate system. The black coordinate represents the aircraft coordinate system.**

33 Two coordinate systems are involved in the calculation of the geo-referenced wind vector: aircraft coordinate system
 34 (black in Figure S1, X , positive forward, Y , to port, and Z , toward the airplane's roof) and geographic coordinate system
 35 (green in Fig. S1, E , positive eastward, N , northward, and U , upward). A transformation matrix, which is defined by
 36 measurements of the three conventional attitude angles: roll (φ), pitch (θ), and heading (ψ), accomplished rotation from the
 37 aircraft to the geographic coordinate. They must be applied in the following order: roll, pitch, and heading to convert from
 38 aircraft coordinate to geographic coordinate, and yaw, pitch, roll to convert the other way. The probe need not be at the
 39 origin of coordinate system. Based on the basic aircraft kinematics and the wind equation given by Lenschow (1986),
 40 considering the influence of tangential velocity of rotation on the probe tip, the full expression to compute the geo-
 41 referenced wind by aircraft can be expressed as:

$$42 \quad U(t) = G(t)\hat{U}_a(t) + U_p(t) + \Omega_p(t) \times R_p \quad (S2)$$

43 The unadorned symbols in Eq. (A2) are in geographic coordinate. The aircraft's coordinate is denoted by ("^"). G is the
 44 transformation matrix. Ω_p is the angular rate of the aircraft. The components of \hat{U}_a are measured with the 5HP mounted on
 45 the nose of the UAV, usually extended on the forward part of the aircraft to reduce the measurable effects of the airflow
 46 distortion by the wing. The components of G , U_p and Ω_p are obtained from the integrated navigation system (INS) outputs,
 47 which originate from the center of gravity (CG) of the UAV. R_p is the vector distance from the CG of the UAV to the 5HP
 48 tip.

49 The rotation matrix G from airplane to earth coordinates is computed in factored form by sequentially removing the
 50 dependence of the observed data on roll, pitch, and heading together with a relabeling of axes. The first rotation $T_1(\varphi)$
 51 removes roll: it is a rotation about the X -axes with matrix representation:

$$52 \quad T_1(\varphi) = \begin{bmatrix} 1 & 0 & 0 \\ 0 & \cos\varphi & -\sin\varphi \\ 0 & \sin\varphi & \cos\varphi \end{bmatrix} \quad (S3)$$

53 The next rotation $T_2(\theta)$ removes pitch:

$$54 \quad T_2(\theta) = \begin{bmatrix} \cos\theta & 0 & \sin\theta \\ 0 & 1 & 0 \\ -\sin\theta & 0 & \cos\theta \end{bmatrix} \quad (S4)$$

55 The last rotation $T_3(\psi)$ removes heading:

$$56 \quad T_3(\psi) = \begin{bmatrix} \cos\psi & -\sin\psi & 0 \\ \sin\psi & \cos\psi & 0 \\ 0 & 0 & 1 \end{bmatrix} \quad (S5)$$

57 The present coordinates of the hypothetical aircraft frame point north, east, and down, and must be transformed to east,
58 north and up. This is done with the permutation T_4 :

$$59 \quad T_4 = \begin{bmatrix} 0 & 1 & 0 \\ 1 & 0 & 0 \\ 0 & 0 & -1 \end{bmatrix} \quad (S6)$$

60 Then, the total transformation G between the frames is the matrix product:

$$61 \quad G = T_4 T_3(\psi) T_2(\theta) T_1(\varphi) = \begin{bmatrix} \sin\psi \cos\theta & \cos\psi \cos\varphi + \sin\psi \sin\theta \sin\varphi & \sin\psi \sin\theta \cos\varphi - \cos\psi \sin\varphi \\ \cos\psi \cos\theta & -\sin\psi \cos\varphi + \cos\psi \sin\theta \sin\varphi & \sin\psi \sin\varphi + \cos\psi \sin\theta \cos\varphi \\ \sin\theta & -\cos\theta \sin\varphi & \cos\theta \cos\varphi \end{bmatrix} \quad (S7)$$

62 In addition, offset corrections ($\varepsilon_\varphi, \varepsilon_\theta, \varepsilon_\psi$) are introduced here to correct for possible misalignment of the CG to the
63 probe's relative wind sensors. The generally small values of these correction constants are determined via dedicated flight
64 maneuvers (in Text 2). Due to the offset in φ had an insignificant effect on the computed wind speed (Van Den Kroonenberg
65 et al., 2008), therefore, ε_φ was not included in the calibration and was set to 0. Then, the three-rotation angle could be
66 expressed as:

$$67 \quad \begin{cases} \varphi = \varphi_i \\ \theta = \theta_i + \varepsilon_\theta \\ \psi = \psi_i + \varepsilon_\psi \end{cases} \quad (S8)$$

68 where $\varphi_i, \theta_i,$ and ε_ψ are the INS measured attitude angle.

69 The cross-product term ($\Omega_p \times R_p$) in Eq. (S2) describe the ‘‘lever arm’’ effect due to the tip of the 5HP not being placed at
70 the CG of the UAV, and all are defined in earth coordinates. In the UAV, the displacement of the 5HP tip with respect to the
71 CG of the UAV along the X-axis ($L = 1.459$ m) is larger than the displacement along the Y-axis (0 m), and Z-axis (0.173 m),
72 so that the lateral and vertical separation distances can be negligible. Then, R_p can be expressed as:

$$73 \quad R_p = G(t) \cdot \begin{bmatrix} L \\ 0 \\ 0 \end{bmatrix} = \begin{bmatrix} L \cos \psi \cos \theta \\ L \sin \psi \cos \theta \\ -L \sin \theta \end{bmatrix} \quad (S9)$$

74 Similarly, Ω_p can be expressed as:

$$75 \quad \Omega_p = \begin{bmatrix} 0 \\ 0 \\ \dot{\psi} \end{bmatrix} + \begin{bmatrix} \cos \psi & -\sin \psi & 0 \\ \sin \psi & \cos \psi & 0 \\ 0 & 0 & 1 \end{bmatrix} \cdot \begin{bmatrix} 0 \\ \dot{\theta} \\ 0 \end{bmatrix} + \begin{bmatrix} \cos \psi \cos \theta & -\sin \psi & \cos \psi \sin \theta \\ \sin \psi \cos \theta & \cos \psi & \sin \psi \sin \theta \\ -\sin \theta & 0 & \cos \theta \end{bmatrix} \cdot \begin{bmatrix} \dot{\phi} \\ 0 \\ 0 \end{bmatrix} = \begin{bmatrix} -\dot{\theta} \sin \psi + \dot{\phi} \cos \psi \cos \theta \\ \dot{\theta} \cos \psi + \dot{\phi} \sin \psi \cos \theta \\ \dot{\psi} - \dot{\phi} \sin \theta \end{bmatrix} \quad (S10)$$

76 Thus,

$$77 \quad \Omega_p \times R_p = T_4 L \begin{bmatrix} -\dot{\theta} \sin \theta \cos \psi - \dot{\psi} \sin \psi \cos \theta \\ \dot{\psi} \cos \psi \cos \theta - \dot{\theta} \sin \psi \sin \theta \\ -\dot{\theta} \cos \theta \end{bmatrix} \quad (S11)$$

78 Then, converting to a meteorological and inertial navigation frame of reference:

$$79 \quad \Omega_p \times R_p = L \begin{bmatrix} \dot{\psi} \cos \psi \cos \theta - \dot{\theta} \sin \psi \sin \theta \\ -\dot{\theta} \sin \theta \cos \psi - \dot{\psi} \sin \psi \cos \theta \\ \dot{\theta} \cos \theta \end{bmatrix} \quad (S12)$$

80 where $\dot{\psi}$ and $\dot{\theta}$ are the angular velocity of heading (ψ) and pitch (θ) angle. The air velocity component (\hat{U}_a) with respect
81 to the aircraft is measured by 5HP. Generally, wind measurements by aircraft are subject to flow distortion and needed to be
82 corrected. According to Vellinga et al. (2013) and Crawford et al. (1996), considering the influence of lift-induced upwash,
83 the wind components with respect to the aircraft ($\hat{u}_a, \hat{v}_a, \hat{w}_a$), can be calculated as:

$$84 \quad \hat{U}_a = \begin{bmatrix} \hat{u}_a \\ \hat{v}_a \\ \hat{w}_a \end{bmatrix} = \frac{|U_a|}{D} \begin{bmatrix} -1 \\ \tan \beta \\ \tan \alpha \end{bmatrix} + w_u \begin{bmatrix} \sin \chi \\ 0 \\ -\cos \chi \end{bmatrix} \quad (S13)$$

$$85 \quad D = (1 + \tan^2 \alpha + \tan^2 \beta)^{1/2} \quad (S14)$$

86 where $|U_a|$ is the magnitude of the true airspeed, α is the angle of attack (the airstream with respect to the aircraft in the
87 aircraft's vertical plane, with positive in the downward direction), β is the angle of sideslip (the angle of the airstream with
88 respect to the aircraft in the aircraft's horizontal plane, with clockwise positive rotation), w_u is the vortex's tangential
89 velocity experienced at the probe tip (i.e., lift-induced upwash), and χ is the vertical separation angle probe to wing
90 (Vellinga et al., 2013). For the UAV applications, the influence of flow distortion effects always be ignored because the
91 probe is long enough to avoid the influence of the flow distortion. For the measurement of true airspeed, the details of
92 converting the pressures (static and dynamic) and total air temperature measured by the 5-hole probe (5HP) to the magnitude
93 of the relative true airspeed were given in Sun et al. (2021). Lastly, integrating the equations above, the final geo-referenced
94 wind vectors (u, v, w) are:

$$\begin{aligned}
95 \quad u &= u_p - |U_a|D^{-1}[\sin\psi\cos\theta + \tan\beta(\cos\psi\cos\phi + \sin\psi\sin\theta\sin\phi) + \tan\alpha(\sin\psi\sin\theta\cos\phi - \cos\psi\sin\phi)] - \\
96 \quad &L(\dot{\theta}\sin\theta\sin\psi - \dot{\psi}\cos\psi\cos\theta) \tag{S15}
\end{aligned}$$

$$\begin{aligned}
97 \quad v &= v_p - |U_a|D^{-1}[\cos\psi\cos\theta - \tan\beta(\sin\psi\cos\phi - \cos\psi\sin\theta\sin\phi) + \tan\alpha(\cos\psi\sin\theta\cos\phi + \sin\psi\sin\phi)] - \\
98 \quad &L(\dot{\psi}\sin\psi\cos\theta + \dot{\theta}\cos\psi\sin\theta) \tag{S16}
\end{aligned}$$

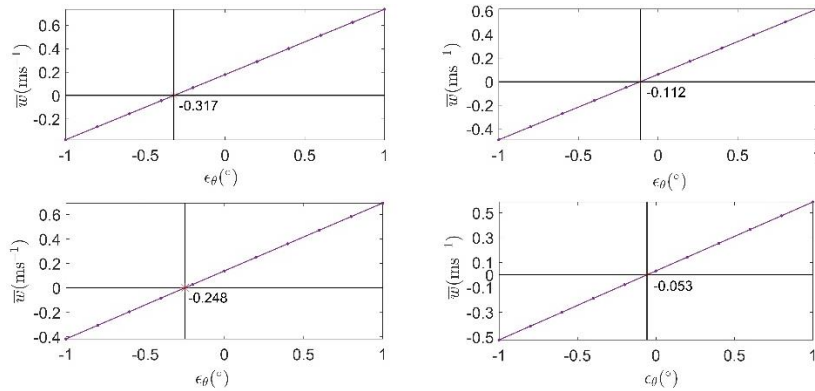
$$99 \quad w = w_p - |U_a|D^{-1}[\sin\theta - \tan\beta\cos\theta\sin\phi - \tan\alpha\cos\theta\cos\phi] + L\dot{\theta}\cos\theta \tag{S17}$$

100 The last term on the right-hand of Eqs. S15-S17 is the leverage effect correction term.

101 2 Calibration results of the ‘box’ flight maneuver

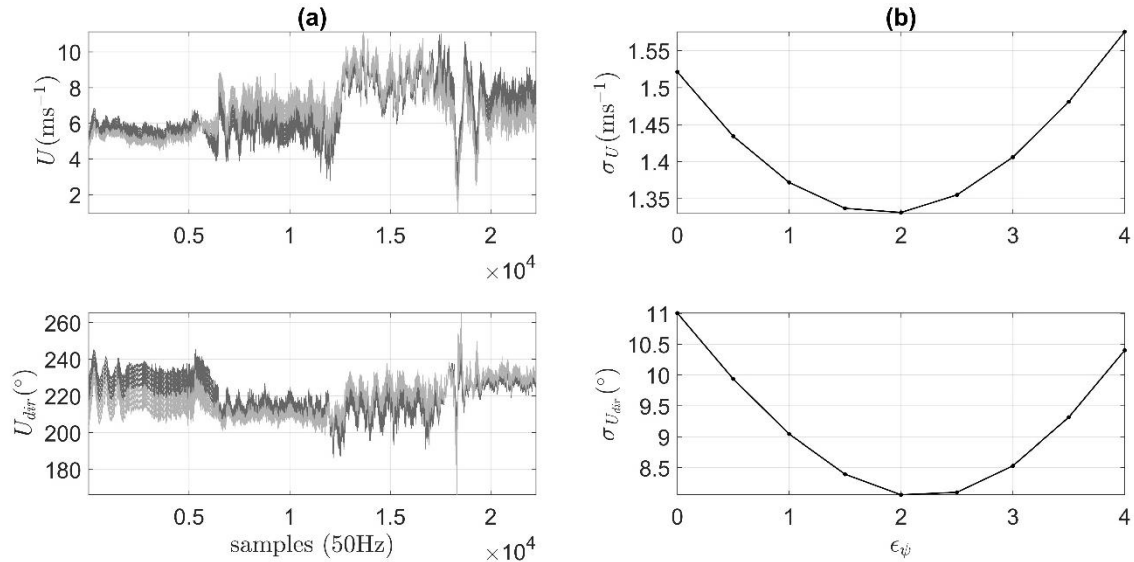
102 In our calibration flight campaign, the first ‘box’ flight maneuver was used to correct the mounting misalignment in heading
103 (ϵ_ψ) and pitch (ϵ_θ) angles between the 5HP and the CG of the UAV. The offset in roll angle (ϵ_ϕ) was not included in the
104 calibration and was set to 0° since its influence on the wind calculation is minimal. The detailed procedure for acquiring the
105 calibration parameter ϵ_ψ and ϵ_θ are given in Vellinga et al. (2013) and Sun et al. (2021). The calibration of the UAV-based
106 EC system should occur in ideal atmospheric conditions, i.e., a constant mean horizontal wind component, near zero mean
107 vertical wind. During the calibration, only the data from the straight sections of the ‘box’ flight maneuver were used. The
108 calibration values ϵ_ψ and ϵ_θ were both determined iteratively until their values reached a steady state.

109 Before calibration, ϵ_ψ and ϵ_θ were set to their default value (0°). The offset ϵ_θ was first calibrated. The value of ϵ_θ was set
110 to vary within the typical range of $\pm 1^\circ$, and the mean vertical wind component (\bar{w}) was iteratively calculated using a step
111 length of 0.2° to find the value of ϵ_θ for which \bar{w} is zero. The individual straight sections of the ‘box’ maneuver are used.
112 The results are shown in Figure S2. The average offset was calculated and served as the final value used in Eq. 8. The final
113 iterative step resulted in an offset of -0.183° for ϵ_θ .



114
115 **Figure S2. Offset values (ϵ_θ) in the pitch angle corresponding to the zero-averaged value of the vertical wind component ($\bar{w} = 0$).**
116 **The final offset value (ϵ_θ) in the pitch angle was calculated by averaging the determined offset value from the individual straight**
117 **sections of the ‘box’ maneuver.**

118 Next, the offset ϵ_ψ was calibrated by setting the possible value to vary within the range between 0° and 4° and by
 119 iteratively calculating the horizontal wind speed using a step length of 0.5° . The final offset ϵ_ψ was determined from the
 120 straight sections of the ‘box’ maneuver by finding the minimum variances for horizontal wind direction ($\sigma_{U_{dir}}$) and wind
 121 speed velocity (σ_U). Figure S3 shows the results for ϵ_ψ from the final iterative session of the calibration. Figure S3b shows
 122 that $\sigma_{U_{dir}}$ and σ_U reach their minima at the offset value of 1.822° and 2.178° , respectively. The final offset value ϵ_ψ is
 123 determined as their average of 2° .



124

125 **Figure S3. Offset values (ϵ_θ) in the pitch angle corresponding to the zero-averaged value of the vertical wind component ($\bar{w} = 0$).**
 126 **The final offset value (ϵ_θ) in the pitch angle was calculated by averaging the determined offset value from the individual straight**
 127 **sections of the ‘box’ maneuver.**

128 References

- 129 Crawford, T. L. and Dobosy, R. J.: A sensitive fast-response probe to measure turbulence and heat flux from any airplane,
 130 Boundary-Layer Meteorology, 59, 257-278, 10.1007/BF00119816, 1992.
- 131 Khelif, D., Burns, S. P., and Friehe, C. A.: Improved Wind Measurements on Research Aircraft, Journal of Atmospheric and
 132 Oceanic Technology, 16, 860-875, 10.1175/1520-0426(1999)016<0860:IWMORA>2.0.CO;2, 1999.
- 133 Lenschow, D. H.: Aircraft Measurements in the Boundary Layer, in: Probing the Atmospheric Boundary Layer, edited by:
 134 Lenschow, D. H., American Meteorological Society, Boston, MA, Boston, https://doi.org/10.1007/978-1-944970-14-7_5,
 135 1986.
- 136 Metzger, S., Junkermann, W., Butterbach-Bahl, K., Schmid, H. P., and Foken, T.: Measuring the 3-D wind vector with a
 137 weight-shift microlight aircraft, Atmos. Meas. Tech., 4, 1421-1444, 10.5194/amt-4-1421-2011, 2011.

138 Sun, Y., Ma, J., Sude, B., Lin, X., Shang, H., Geng, B., Diao, Z., Du, J., and Quan, Z.: A UAV-Based Eddy Covariance
139 System for Measurement of Mass and Energy Exchange of the Ecosystem: Preliminary Results, *Sensors*, 21,
140 10.3390/s21020403, 2021.

141 van den Kroonenberg, A., Martin, T., Buschmann, M., Bange, J., and Vörsmann, P.: Measuring the Wind Vector Using the
142 Autonomous Mini Aerial Vehicle M2AV, *Journal of Atmospheric and Oceanic Technology*, 25, 1969-1982,
143 10.1175/2008JTECHA1114.1, 2008.

144 Vellinga, O. S., Dobosy, R. J., Dumas, E. J., Gioli, B., Elbers, J. A., and Hutjes, R. W. A.: Calibration and Quality Assurance
145 of Flux Observations from a Small Research Aircraft*, *Journal of Atmospheric and Oceanic Technology*, 30, 161-181,
146 10.1175/JTECH-D-11-00138.1, 2013.

147 Williams, A. and Marcotte, D.: Wind Measurements on a Maneuvering Twin-Engine Turboprop Aircraft Accounting for
148 Flow Distortion, *Journal of Atmospheric and Oceanic Technology*, 17, 795-810, 10.1175/1520-
149 0426(2000)017<0795:WMOAMT>2.0.CO;2, 2000.

150